DOI: 10.1002/cbic.200800524

Structural Effects on ss- and dsDNA Recognition by a β-Hairpin Peptide

Amanda L. Stewart and Marcey L. Waters*[a]

The interactions involved in the binding of a designed β-hairpin dimer to single-stranded and duplex DNA have been explored. Previously the peptide dimer had been found to bind ssDNA with a dissociation constant of 3 μM through a combination of aromatic and electrostatic interactions, whereas binding to duplex DNA was primarily driven by electrostatic interactions. In this report, the effects of folding and chirality were studied to determine the factors that contribute to affinity and selectivity for ssDNA versus dsDNA. Binding studies showed that 1) folding is crucial for binding to both ss- and dsDNA, and 2) chirality affects binding for duplex DNA but not for ssDNA. Taken together, these studies reveal different modes of binding for ss- and duplex DNA, with different driving forces, but in each case peptide structure contributes significantly to binding.

Introduction

Protein–DNA interactions are involved in a variety of biological processes such as transcription, translation, and DNA repair. Protein interactions with single-stranded DNA (ssDNA) are particularly critical in DNA recombination, replication, and repair,[1–3] telomere regulation,[4] and cold shock response.[5] Proteins recognize ssDNA through a combination of electrostatic, aromatic, and hydrogen-bonding interactions. Almost all proteins recognize ssDNA through an OB-fold domain (oligonucleotide/oligosaccharide binding fold),[2–3] which is a solvent-exposed β-sheet surface composed of two three-stranded antiparallel β-sheets that form a five-stranded β-barrel in which the first strand is in both sheets (Figure 1).[2,5a] Replication protein A (RPA)[1,3] and cold shock protein[5] are well studied examples of proteins containing single-stranded DNA binding domains. This laboratory has designed a β-hairpin peptide dimer that functions as a minimalist mimic of the OB-fold for recognition of ssDNA.[6] This peptide was designed to recognize nucleic acids and to determine the favorable interactions that provide affinity and selectivity for recognition of ssDNA. In this study, the contributions of β-hairpin structure and chirality to binding affinity and selectivity for ssDNA and double-stranded DNA (dsDNA) were investigated.

Figure 1. Structure of the *Bacillus caldolyticus* cold shock protein bound to oligothymidine (PDB ID: 2hax; top).[5a] The aromatic side chains involved in binding are explicitly shown.

Originally, the peptide WKWK (Scheme 1 A) was designed to bind nucleotides through a binding cleft of two tryptophan residues and two flanking cationic lysine residues. The name of the peptide reflects the residues on the binding face of the β-hairpin. It was shown by fluorescence quenching of the tryptophan residues to bind ATP with a K_d value of 170 μM.[7] Through a combination of salt studies, mutation studies, and NMR and circular dichroism (CD) investigations of the peptide–ATP complex, the binding mode of WKWK was characterized. Binding was found to be driven by both aromatic and electrostatic interactions. Aromatic interactions between the nucleobase and the cleft made up of the two Trp side chains were found to contribute about 2 kcal mol^{-1} to binding, whereas electrostatic interactions between the triphosphate and basic residues on the peptide were found to contribute about 3 kcal mol^{-1}.[7]

Dimerization of WKWK through a disulfide bond to give $(WKWK)_2$ (Scheme 1 B) provided two aromatic pockets for binding to oligonucleotides. $(WKWK)_2$ was shown to bind a single-stranded 11 mer (Scheme 1 E) with a K_d value of 3 μM in 10 mM sodium phosphate buffer (100 mM NaCl, pH 7.0) at 298 K.[6]

[a] *A. L. Stewart, Dr. M. L. Waters*
Department of Chemistry, CB 3290, University of North Carolina
Chapel Hill, North Carolina 27599 (USA)
Fax: (+1) 919-962-2388
E-mail: mlwaters@email.unc.edu

Supporting information for this article is available on the WWW under http://www.chembiochem.org or from the author.

 © 2009 Wiley-VCH Verlag GmbH & Co. KGaA, Weinheim

A) **WKWK**: Ac-Arg-**Trp**-Val-**Lys**-Val-Asn-Gly-Orn-**Trp**-Ile-**Lys**-Gln-NH_2

B) **$(WKWK)_2$**:
(Ac-Cys-Gly-Arg-**Trp**-Val-**Lys**-Val-Asn-Gly-Orn-**Trp**-Ile-**Lys**-Gln-$NH_2)_2$

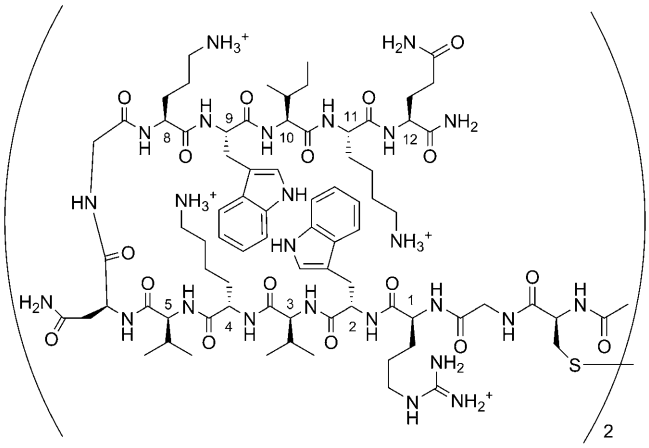

C) **$(WKWK\text{-}N6P)_2$**:
(Ac-Cys-Gly-Arg-**Trp**-Val-**Lys**-Val-Pro-Gly-Orn-**Trp**-Ile-**Lys**-Gln-$NH_2)_2$

D) **$(D\text{-}WKWK)_2$**:
(Ac-DCys-Gly-DArg-D**Trp**-DVal-D**Lys**-DVal-DAsn-Gly-DOrn-D**Trp**-DIle-D**Lys**-DGln-$NH_2)_2$

E) 5'-CCATCGCTACC-3'

F) 5'-CCATCGCTACC-3'
3'-GGTAGCGATGG-5'

Scheme 1. A) β-Hairpin sequence WKWK. The bold residues are those thought to be involved in the nucleic acid binding pocket. Those residues are all on the same face of the peptide. B) Sequence and structure of peptide $(WKWK)_2$. C–D) Mutations to $(WKWK)_2$ with specific mutations underlined. E) ssDNA sequence. F) dsDNA sequence.

This binding affinity is comparable to that found in the cold shock protein A ($K_d \sim 6$ μM), which consists of a single OB-fold.[5b] Binding of $(WKWK)_2$ to a duplex DNA strand of the same length (Scheme 1 F) was found to display similar affinity ($K_d \sim 5$–9 μM),[8] despite the doubling of the negative charge. Studies have shown that aromatic interactions between $(WKWK)_2$ and the unpaired bases in ssDNA provide selectivity over dsDNA under high-salt conditions in which the electrostatic interactions are screened.[6] In duplex DNA, the bases are packed inside the duplex and are not accessible to stacking with residues in the peptide. The preference for ssDNA over dsDNA at physiological salt levels is thus modest, but it is a starting point for a system to improve selectivity for ssDNA over the duplex structure. These studies aimed to explore the modes of binding to ss- and dsDNA by the hairpin dimer to provide insight into approaches for optimizing selectivity.

Results and Discussion

Sequence design

The peptide $(WKWK\text{-}N6P)_2$ (Scheme 1 C), based on the previously reported β-hairpin dimer $(WKWK)_2$, was designed to investigate the importance of structure to binding. Replacement of the Asn residue in the turn with L-Pro has been shown to disrupt the turn and to prevent folding into a β-hairpin structure.[9] This allows us to probe directly whether the aromatic cleft in the β-hairpin contributes to binding.

A second peptide, $(D\text{-}WKWK)_2$ (Scheme 1 D), was synthesized with all D-amino acids to determine the importance of chirality in binding. While $(WKWK)_2$ has a right-handed twist—as do all β-hairpins with all L-amino acids—$(D\text{-}WKWK)_2$ takes on a left-handed twist. Whether the macromolecular chirality of the peptide influences the binding affinity will depend on the mode of binding to ss- and dsDNA.

Characterization of structure

Circular dichroism spectra were obtained to verify the secondary structure of each of the mutants studied. The parent peptide, $(WKWK)_2$, has a characteristic β-sheet spectrum with a minimum at 210 nm (Figure 2). This is consistent with previous

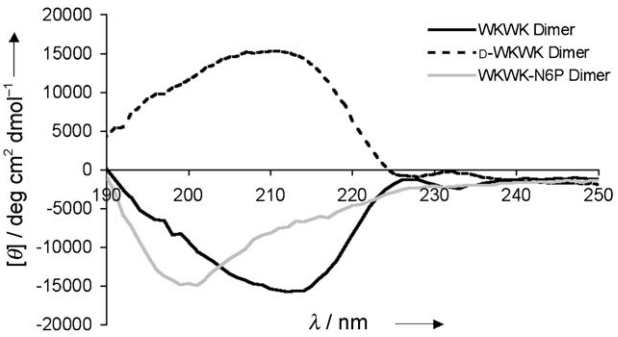

Figure 2. CD data for WKWK dimer and mutants. Data were obtained at 30 μM peptide in Na_2HPO_4 (10 mM), pH 7.0, 298 K. D-WKWK dimer indicates the dimer with all D-amino acids.

NMR data, which indicated that both the monomer and the dimer have high β-hairpin populations under physiological conditions.[6–7] The CD spectra of $(WKWK\text{-}N6P)_2$ verified that it is unstructured, with a minimum at about 200 nm (Figure 2). The CD spectrum of $(D\text{-}WKWK)_2$, containing all D-amino acids, showed the expected signal for the enantiomer of the parent peptide $(WKWK)_2$, with a positive peak at 210 nm indicating a D-peptide with β-sheet structure (Figure 2).

Binding measurements

Binding of ssDNA and duplex DNA to each of the peptides was determined by quenching of the Trp fluorescence as described in the Experimental Procedures. A correction for the inner filter effect arising from absorbance of the nucleobases at the excitation wavelength of Trp was performed for all binding data except for the binding of $(WKWK\text{-}N6P)_2$ to duplex DNA, where binding was weak (see Experimental Procedures). In this case, the inner filter effect was too large to correct for, so the reported dissociation constant is uncorrected and represents a lower limit. In the case of $(WKWK\text{-}N6P)_2$, CD mixing experiments were also performed to confirm that folding of

 © 2009 Wiley-VCH Verlag GmbH & Co. KGaA, Weinheim

the peptide was not induced upon binding (see the Supporting Information).

The stoichiometry of binding was determined for $(WKWK)_2$ by fluorescence quenching by using the molar variation method (see the Experimental Section). A 1:1 binding stoichiometry for the interaction between $(WKWK)_2$ and the 11-mer ssDNA sequence (Scheme 1 E) was determined (see the Supporting Information), in agreement with the stoichiometry reported for the $(WKWK)_2$ interaction with dA_5.[6] The binding stoichiometry for the interaction between $(WKWK)_2$ and the duplex DNA sequence (Scheme 1 F) was also found to be 1:1 (see the Supporting Information).

Influence of folding on binding

To probe the importance of the aromatic pocket in the β-hairpin dimer, we measured binding of the unstructured peptide—$(WKWK\text{-}N6P)_2$—to ss- and dsDNA. In both cases, binding was significantly weaker than with $(WKWK)_2$ (Figures 3 and 4 A, Table 1). Binding is nearly ten times worse for both ssDNA and dsDNA.[10] However, evidence suggests that the reasons for the loss of binding upon disruption of β-hairpin structure differ for ss- and for dsDNA. In the case of ssDNA, the decrease in binding affinity associated with loss of structure is consistent with previous data indicating that the interaction of ssDNA with the β-hairpin is mediated by stacking interactions with the aromatic pocket.[6]

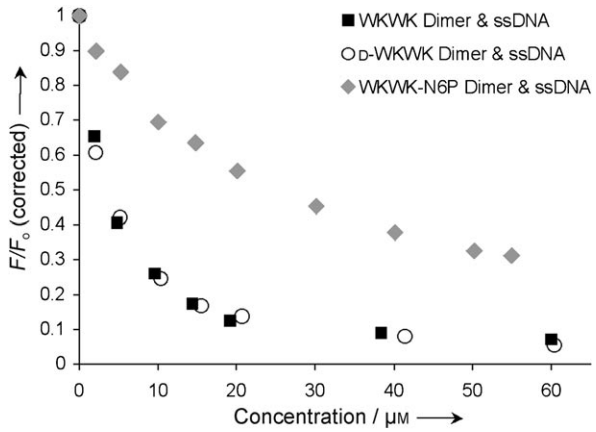

Figure 3. Fluorescence titrations of $(WKWK)_2$ and mutant peptide dimers with the single-stranded DNA sequence 5′-CCATCGCTACC-3′ (Scheme 1 E) corrected for the inner filter effect (see Experimental Section): peptide (2–8 μM), sodium phosphate buffer (10 mM), NaCl (100 mM), pH 7.0, 298 K. "D-WKWK dimer" indicates the dimer with all D-amino acids.

As for dsDNA, the role of structure on binding is less clear. The influence of folding on binding is surprising given that previous studies indicated that binding of $(WKWK)_2$ is primarily electrostatic in nature. Differences in charge density of the folded and unfolded peptides or differences in the entropic cost of binding may play a role. Another possibility is that binding might occur in a structurally defined manner, such as groove binding.

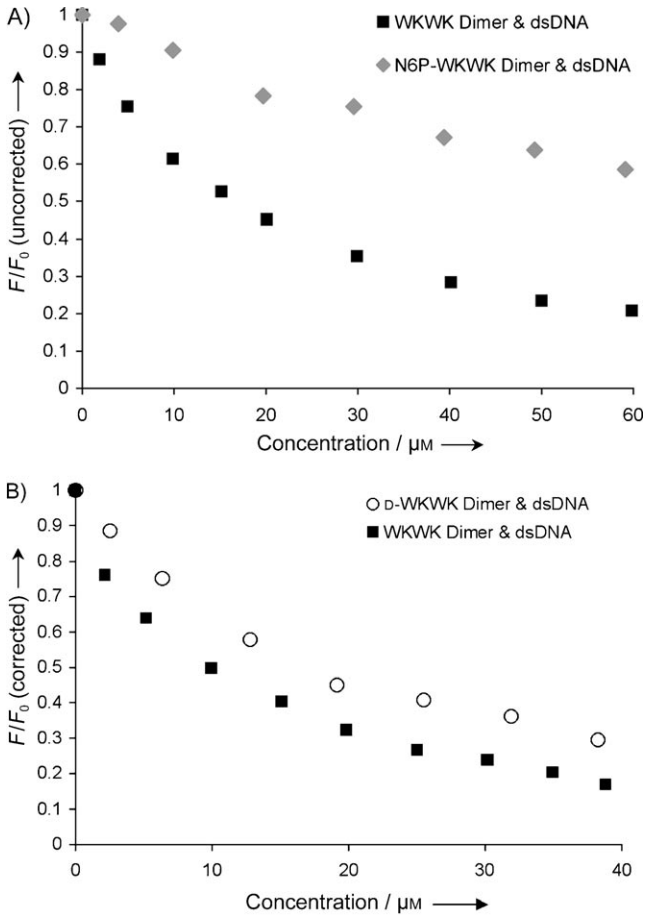

Figure 4. Fluorescence titrations of $(WKWK)_2$ and mutant peptide dimers with duplex DNA (Scheme 1 F): peptide (2–7 μM), sodium phosphate buffer (10 mM), NaCl (100 mM), pH 7.0, 298 K. A) $(WKWK)_2$ and $(WKWK\text{-}N6P)_2$ uncorrected for the inner filter effect. B) $(WKWK)_2$ and $(D\text{-}WKWK)_2$ corrected for the inner filter effect (see the Experimental Section). "D-WKWK dimer" indicates the dimer with all D-amino acids.

Table 1. Affinity constants for binding of peptide dimers to ssDNA and dsDNA sequences.[a]

Peptide	K_d (error) [μM] ssDNA	K_d (error) [μM] dsDNA
$(WKWK)_2$	3.5 (0.2)	9.2 (0.9)[b]
$(WKWK\text{-}N6P)_2$	24.7 (1.6)	~80[c]
$(D\text{-}WKWK)_2$	3.4 (0.2)	17.5 (1.3)

[a] Conditions: sodium phosphate buffer (10 mM), NaCl (100 mM), pH 7.0, 298 K. Each value is the average of at least two measurements. The error is from the fitting. [b] This K_d value was previously reported as 5 μM. See ref. [6]. [c] This value is not corrected for the inner filter effect and thus is only approximate.[10]

Influence of chirality on binding

Because the peptide structure is important to binding, the chirality of the peptide might be important as well. In particu-

 © 2009 Wiley-VCH Verlag GmbH & Co. KGaA, Weinheim

lar, it may be more important in binding to duplex DNA, due to its macromolecular chirality arising from the double helix, than to single-stranded DNA, which is unstructured.

Fluorescence binding studies of the all D-amino acid peptide (D-WKWK)$_2$ to ssDNA gave binding affinities identical to those of its enantiomer (Table 1, Figure 3). In the case of ssDNA, with no macromolecular structure, this suggests that the ribose ring is not directly involved in binding. This is reminiscent of the binding mode of cold shock protein and ssDNA, in which the ribose rings are solvent-exposed and are not in direct contact with the protein (Figure 1).[5a] The fact that the all D-peptide binds with equal affinity to the ssDNA sequence is also significant, because all D-peptides typically display enhanced resistance to cleavage by proteases.[11]

In contrast to its binding to ssDNA, the enantiomeric peptide dimer (D-WKWK)$_2$ binds to duplex DNA with a somewhat weaker affinity than does (WKWK)$_2$ (Figure 4 B). Chirality thus has some influence on binding to duplex DNA, unlike to ssDNA. For duplex DNA, the small but measurable difference in the binding affinities of the L- and D-peptides indicates that the diastereomeric complexes are of different stabilities. This is consistent with the finding that folding influences binding of the parent peptide to dsDNA and provides further support for a structurally defined binding event such as groove binding, in which the twist of the hairpin would be expected to influence its binding affinity.

Structural models for binding ss- and dsDNA

The studies performed here, in conjunction with our previous studies, are consistent with a binding model in which ssDNA interacts with the hairpin dimer through a combination of aromatic and electrostatic interactions defined by the secondary structure of the peptide. In the parent peptide—(WKWK)$_2$—recognition of ssDNA is approximately 1.5 to three times more favorable than recognition of duplex DNA, despite the fact that the net charge on the duplex is twice that of the single-stranded oligonucleotide. This selectivity is attributed to aromatic interactions between the unpaired bases and the aromatic cleft in the β-hairpin.[6] Disruption of the hairpin structure results in a reduction in binding affinity of nearly tenfold and is attributed to loss of the aromatic pocket. Because the ssDNA is unstructured, the chirality of the peptide does not influence binding. (D-WKWK)$_2$ thus provides selectivity for ssDNA over dsDNA by a factor of five.

The binding mode for duplex DNA is quite different. Previous studies indicated that binding is primarily electrostatic in nature,[6] suggesting nonspecific binding, as has been observed with unstructured cationic peptides.[12] However, the importance of both folding and chirality for binding provides a more complex picture. These studies suggest that binding occurs through a structurally defined complex, likely involving groove binding of the hairpin to the duplex DNA. In this case, the Trp side chains may simply provide a well folded structure or may supply hydrophobic contacts in the major groove (alternatively, the aliphatic side chains on the opposite face of the hairpin may provide such contacts).

Groove binding by a β-hairpin is not unprecedented in protein–DNA interactions; binding of β-hairpins within the major groove of duplex DNA has been observed in a number of protein–DNA complexes such as those shown in Figure 5.[13] A β-hairpin, for example, is key in recognizing the target sequence GCC-box in the GCC-box binding domain of AtERF1 (Figure 5 A).[13a] The GCC-box binding domain (GBD) binds to the major groove of the GCC-box through a three-stranded β-sheet and an α-helix. The β-sheet enters into extensive interactions with the DNA, with arginine and tryptophan residues recognizing the DNA and forming contacts with eight base pairs in the major groove. Arg and Trp also bind the sugar phosphate backbone. The α-helix is known to make only one contact with the DNA, binding a phosphate group. Interestingly, the binding of GBD to DNA is similar to binding by zinc finger proteins, except that the α-helix that binds to the major groove in the zinc finger is replaced by the β-hairpin in GBD.[13a]

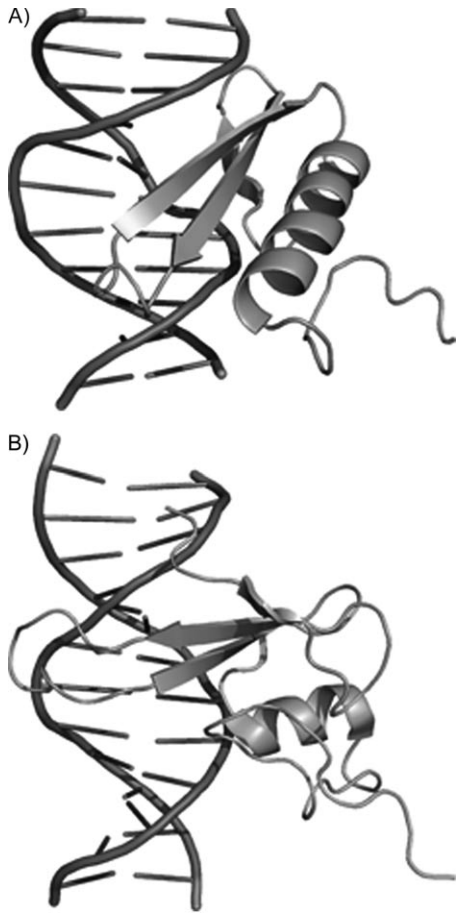

Figure 5. Protein–DNA complexes of A) the GCC-box binding domain of AtERF1 (PDB ID: 1gcc),[13a] and B) the methyl-CpG-binding domain of human MBD1 (PDB ID: 1ig4).[13b]

In the human methylation-dependent transcriptional regulator methyl-CpG binding domain 1 (MBD1), a hairpin loop forms several contacts deep within the major groove near the methylated DNA site (Figure 5 B).[13b] Specific recognition of the

 © 2009 Wiley-VCH Verlag GmbH & Co. KGaA, Weinheim

methylated bases is mediated by two arginine residues, a tyrosine residue, and an aspartic acid residue. Side chain–side chain interactions seem to play an important role in binding, because mutations of the Asp residue weaken DNA binding despite its lack of direct contact with the DNA.[13b]

The *Chlorella* virus DNA ligase recognizes nicked DNA through a β-hairpin loop that stems from an OB-fold domain to form a latch that binds the major groove flanking the nick. The OB-fold domain binds the minor groove behind the nick.[14] The homing endonuclease I-SceI in yeast also recognizes DNA primarily through interactions with a long β-hairpin loop that extends into the major groove of the duplex DNA.[15]

There are recent examples of designed β-hairpin peptides that bind to RNA,[16] but to the best of our knowledge this peptide is the only example of a designed β-hairpin that binds to duplex DNA. Moreover, there are examples of synthetic β-hairpins that mimic helical protein domains in protein–protein[17] and protein–RNA interactions,[16] but not in DNA. Our findings suggest that β-hairpins may be promising mimics for α-helical DNA binding domains. This is appealing in that β-hairpins provide more robust structures than α-helices and can easily be cyclized to reduce entropic costs and to provide increased protease resistance.

Conclusions

In conclusion, these studies provide insight into the factors that contribute to β-hairpin recognition of both ss- and dsDNA, which has relevance to protein receptors for each of these types of DNA. These studies indicate that folding is required for binding of both ss- and dsDNA even though the driving forces for binding them are different. In the case of ssDNA, folding provides an aromatic cleft to form favorable stacking interactions with the nucleobases. In the case of duplex DNA, folding allows for binding in a structure-dependent manner, such as groove binding, through favorable electrostatic interactions. The observed differences in binding suggest approaches to improving selectivity for ss- versus dsDNA with biomimetic receptors.

Experimental Section

Peptide synthesis and purification: Peptides were synthesized by automated solid-phase peptide synthesis with an Applied Biosystems Pioneer Peptide Synthesizer. Fmoc-protected amino acids were used with a PEG-PAL-PS resin. Amino acid residues were activated with HBTU (*O*-benzotriazole-*N*,*N*,*N*′,*N*′,-tetramethyluronium hexafluorophosphate) and HOBT (*N*-hydroxybenzotriazole), together with DIPEA (diisopropylethylamine) in DMF (*N*,*N*-dimethylformamide). Amino acids were deprotected by treatment with DBU (1,8-diazabicyclo[5.4.0]undec-7-ene) (2%) and piperidine (2%) in DMF for approx. 10 min. Each amino acid was coupled in an extended cycle of 75 min to improve coupling. The N terminus of each peptide was acetylated with acetic anhydride (5%) and lutidine (6%) in DMF (30 min). Cleavage of the peptides from the resin was performed in trifluoroacetic acid (TFA, 94%), H_2O (2.5%), ethanedithiol (EDT, 2.5%), and triisopropylsilane (TIPS, 1%) over 3 h. TFA was evaporated by bubbling with nitrogen, and ether was added to the resulting product. The peptide was then extracted with water and lyophilized to a powder.

Peptides were purified by reversed-phase HPLC. A Vydac C-18 semi-preparative column was used for separation with a gradient of solvent B (5–35%) over 25 min with solvent A water/acetonitrile (95:5), TFA (0.1%) and solvent B acetonitrile/water (95:5), TFA (0.1%). Peptides were then lyophilized, and the peptide sequences were confirmed by MALDI mass spectrometry. Peptide dimers were formed by oxidation of the cysteine residues through stirring in DMSO (1%) in phosphate buffer (10 mM), pH 7.5 for 3–7 h. After purification, all peptides were desalted with a Pierce D-Salt Polyacrylamide 1800 desalting column.

DNA sample preparation: Two strands of DNA were purchased from IDT (Integrated DNA Technologies). The strands obtained were 5′-CCATCGCTACC-3′ and its complement. All DNA samples were prepared in triethylammonium acetate (TEAA) buffer [acetic acid (5.6%), triethylamine (TEA, 13.86%) in water, adjusted to pH 7.0]. DNA samples were dissolved in TEAA buffer (1 mL). Buffer was added individually to DNA (1 μmol). The DNA solution was pooled, and additional TEAA buffer (1 mL) was added to each DNA sample. This was then pooled and filtered before purification by reversed-phase HPLC. Purification was performed on the same column as that used for peptides with a gradient of solvent B (25–75%) over 20 min (6 mL min^{-1} flow rate). Solvent A was acetonitrile (5%)/TEAA buffer (95%), and solvent B was acetonitrile (15%)/TEAA buffer (85%). Samples were lyophilized after purification, and the resulting product was then dissolved in water and re-lyophilized to remove any remaining salts. Concentrations of both DNA strands were determined with a Perkin–Elmer Lambda 35 UV/Vis Spectrometer. Absorbance values were determined at 260 nm, and concentrations were calculated from the extinction coefficients of the two DNA strands ($\varepsilon_{260,\,ssDNA} = 95\,500\ M^{-1}cm^{-1}$ and $\varepsilon_{260,\,ssDNA\ complement} = 112\,600\ M^{-1}cm^{-1}$). Equal concentrations of the two strands (in sodium phosphate buffer, pH 7.0) were pooled in a final concentration of NaCl (100 mM). The solution was heated at 95 °C for 5 min to anneal the strands and was then allowed to cool to room temperature before storing at −20 °C.

Circular dichroism: All peptide dimers were analyzed by CD to verify their structures. CD measurements were performed on an Aviv Model 62 DS circular dichroism spectrometer. The peptides (30 μM) were dissolved in Na_2HPO_4 (10 mM), pH 7.0. Wavelength scans were performed at 298 K from 260–185 nm. CD mixing experiments were performed by the same method. Individual peptide and DNA samples had the same concentration (50 μM), and the mixtures contained equal concentrations (50 μM each). Mixing experiments were performed in phosphate buffer (10 mM) containing NaCl (100 mM) because NaCl is required for DNA annealing.

Fluorescence titrations: To determine the recognition of single-stranded and duplex oligonucleotides by the peptide dimers, fluorescence titrations that monitored the Trp quenching with increasing oligonucleotide concentration were performed. Peptide and nucleotide samples were prepared in sodium phosphate buffer (10 mM), NaCl (100 mM), pH 7.0. Peptide concentrations were determined in guanidine hydrochloride (5 M) by recording the absorbance of the Trp residues at 280 nm ($\varepsilon = 5690\ M^{-1}cm^{-1}$) by UV/Vis spectroscopy. Concentrations of nucleotides were determined by UV/Vis spectroscopy by observation of the absorbance at 260 nm. Fluorescence scans were obtained on a Cary Eclipse Fluorescence Spectrophotometer from Varian. Experiments were performed at 298 K with an excitation wavelength of 297 nm. Fluorescence emission intensities of the Trp residues at 348 nm were

 © 2009 Wiley-VCH Verlag GmbH & Co. KGaA, Weinheim

fitted as a function of nucleotide concentration to the binding Equation (1) on Kaleidagraph by nonlinear least-squares fitting.[18]

$$I = \frac{I_o + I_\infty([L]/K_d)}{1 + ([L]/K_d)} \quad (1)$$

where I is the observed fluorescence intensity, I_o is the initial fluorescence intensity of the peptide, I_∞ is the fluorescence intensity at binding saturation, [L] is the concentration of added nucleotide, and K_d is the dissociation constant.

Oligonucleotides display observable absorbance at the excitation wavelength of Trp (297 nm), and so there is an inner filter effect that one must take into account. The absorbance of the oligonucleotides at 297 nm was monitored at known concentrations, and the extinction coefficient was determined. Absorbance values were determined for each oligonucleotide concentration. Corrected fluorescence values were determined from Equations (2) and (3)].[19]

$$F_c = F_o/C_i \quad (2)$$

$$C_i = \frac{1-10^{-A_i}}{2.303\,A_i} \quad (3)$$

where F_c is the corrected fluorescence, F_o is the fluorescence observed, and C_i is the correction factor for each absorbance value (i). A_i is the absorbance value for each concentration determined by the extinction coefficient.

Stoichiometry of binding: The stoichiometry of binding was determined by the molar variation method by monitoring the quenching of tryptophan fluorescence. Conditions were such that the peptide and DNA should be fully bound. Peptide concentrations varied (25–45 μM) depending on the maximum DNA concentrations used. The conditions were limited to low concentrations for ssDNA (~60 μM) and duplex DNA (~40 μM) because of the inner filter effect. After correction for the inner filter effect, the fluorescence intensity was plotted against the ratio of DNA/peptide concentrations to give the stoichiometry of binding. The stoichiometry of binding is shown in plots (Figure S2 and S3 in the Supporting Information) with the x-intercept of the dashed lines indicating the stoichiometry for each.

Acknowledgements

We gratefully acknowledge support for this research from the National Institutes of Health (GM072691).

Keywords: beta-hairpins · DNA binding · molecular recognition · OB-fold domain · protein structures

[1] a) A. Bochkarev, R. A. Pfuetzner, A. M. Edwards, L. Frappier, *Nature* **1997**, *385*, 176–181; b) M. S. Wold, *Annu. Rev. Biochem.* **1997**, *66*, 61–92.
[2] D. L. Theobald, R. M. Mitton-Fry, D. S. Wuttke, *Annu. Rev. Biophys. Biomol. Struct.* **2003**, *32*, 115–133.
[3] A. Bochkarev, E. Bochkareva, *Curr. Opin. Struct. Biol.* **2004**, *14*, 36–42.
[4] a) E. M. Anderson, W. A. Halsey, D. S. Wuttke, *Biochemistry* **2003**, *42*, 3751–3758; b) R. M. Mitton-Fry, E. M. Anderson, T. R. Hughes, V. Lundblad, D. S. Wuttke, *Science* **2002**, *296*, 145–147.
[5] a) K. E. A. Max, M. Zeeb, R. Bienert, J. Balbach, U. Heinemann, *FEBS J.* **2007**, *274*, 1265–1279; b) B. J. Hillier, H. M. Rodriguez, L. M. Gregoret, *Folding Des.* **1998**, *3*, 87–93; c) K. Newkirk, W. Feng, W. Jiang, R. Tejero, S. D. Emerson, M. Inouye, G. T. Montelione, *Proc. Natl. Acad. Sci. USA* **1994**, *91*, 5114–5118; d) H. Schindelin, M. A. Marahiel, U. Heinemann, *Nature* **1993**, *364*, 164–168; e) A. Schnuchel, R. Wiltscheck, M. Czisch, M. Herrier, G. Willimsky, P. Graumann, M. A. Marahiel, T. A. Holak, *Nature* **1993**, *364*, 169–171.
[6] S. M. Butterfield, W. J. Cooper, M. L. Waters, *J. Am. Chem. Soc.* **2005**, *127*, 24–25.
[7] S. M. Butterfield, M. L. Waters, *J. Am. Chem. Soc.* **2003**, *125*, 9580–9581.
[8] The K_d value for $(WKWK)_2$ with the duplex DNA sequence shown in Scheme 1F was determined to be 5 μM in a previous publication, but repeated experiments here give a K_d of 9 μM under the same conditions.
[9] H. E. Stanger, S. H. Gellman, *J. Am. Chem. Soc.* **1998**, *120*, 4236–4237.
[10] Due to the small change in tryptophan fluorescence resulting from weak binding, no accurate dissociation constant could be obtained for the $(WKWK\text{-}N6P)_2$ peptide with dsDNA.
[11] a) K. Hamamoto, Y. Kida, Y. Zhang, T. Shimizu, K. Kuwano, *Microbiol. Immunol.* **2002**, *46*, 741–749; b) R. Tugyi, K. Uray, D. Ivan, E. Fellinger, A. Perkins, F. Hudecz, *Proc. Natl. Acad. Sci. USA* **2005**, *102*, 413–418.
[12] a) D. P. Mascotti, T. M. Lohman, *Biochemistry* **1992**, *31*, 8932–8946; b) D. P. Mascotti, T. M. Lohman, *Biochemistry* **1993**, *32*, 10568–10579.
[13] a) M. D. Allen, K. Yamasaki, M. Ohme-Takagi, M. Tateno, M. Suzuki, *EMBO J.* **1998**, *17*, 5484–5496; b) I. Ohki, N. Shimotake, N. Fujita, J. G. Jee, T. Ikegami, M. Nakao, M. Shirakawa, *Cell* **2001**, *105*, 487–497.
[14] P. A. Nair, J. Nandakumar, P. Smith, M. Odell, C. D. Lima, S. Shuman, *Nat. Struct. Mol. Biol.* **2007**, *14*, 770–778.
[15] C. M. Moure, F. S. Gimble, F. A. Quiocho, *J. Mol. Biol.* **2003**, *334*, 685–695.
[16] a) Z. Athanassiou, K. Patora, R. L. A. Dias, K. Moehle, J. A. Robinson, G. Varani, *Biochemistry* **2007**, *46*, 741–751; b) K. Moehle, Z. Athanassiou, K. Patora, A. Davidson, G. Varani, J. A. Robinson, *Angew. Chem.* **2007**, *119*, 9260–9264; *Angew. Chem. Int. Ed.* **2007**, *46*, 9101–9104; c) T. C. Leeper, Z. Athanassiou, R. L. A. Dias, J. A. Robinson, G. Varani, *Biochemistry* **2005**, *44*, 12362–12372; d) Z. Athanassiou, R. L. A. Dias, K. Moehle, N. Dobson, G. Varani, J. A. Robinson, *J. Am. Chem. Soc.* **2004**, *126*, 6906–6913.
[17] a) R. Fasan, R. L. A. Dias, K. Moehle, O. Zerbe, J. W. Vrijbloed, D. Obrecht, J. A. Robinson, *Angew. Chem.* **2004**, *116*, 2161–2164; *Angew. Chem. Int. Ed.* **2004**, *43*, 2109–2112; b) R. Fasan, R. L. A. Dias, K. Moehle, O. Zerbe, D. Obrecht, P. R. E. Mittl, M. G. Grutter, J. A. Robinson, *ChemBioChem* **2006**, *7*, 515–526.
[18] W. A. Lim, R. O. Fox, F. M. Richards, *Protein Sci.* **1994**, *3*, 1261–1266.
[19] T. M. Lohman, D. P. Mascotti, *Methods Enzymol.* **1992**, *212*, 424–458.

Received: August 1, 2008
Published online on January 14, 2009

 © 2009 Wiley-VCH Verlag GmbH & Co. KGaA, Weinheim